Micromechanical analysis of stress in an unsatured granular medium

R. Wan, S. Khosravani, François Nicot

MICROMECHANICAL ANALYSIS OF STRESS IN AN UNSATURATED GRANULAR MEDIUM

R. Wan & S. Khosravani
Department of Civil Engineering, University of Calgary, Calgary, AB, Canada
F. Nicot
Cemagref, Grenoble, France

ABSTRACT: The paper is concerned with a micromechanical formulation of force transmission within an unsaturated soil as a three-phase system composed of idealized spherical particles connected by a pore water menisci network. It is proposed here a tensorial effective stress equation that can be viewed as a generalized Bishop's equation in which the elusive effective stress parameter χ is elucidated. The latter can be expressed as an explicit function of the number of water menisci, particle packing and degree of water saturation. Also, interparticle forces are found to be dependent on the distribution of pore fluid pressure and the contractile skin arising from the interaction of interfaces. Two major findings of this work are: (1) the determination of the analytical relationship between χ and degree of saturation, and (2) the identification of a suction based internal shear effect even under isotropic external loading. The understanding of suction stress and its dependency on the degree of saturation is a longstanding problem both theoretically and experimentally.

1. INTRODUCTION

Unsaturated soils represent an important three-phase system in which internal forces arise from the interaction of solid, liquid and gas phases. As such, in determining the behaviour and strength of unsaturated soils, it becomes difficult to choose the controlling stress variable that would substitute for the role of effective stress in the saturated case. Bishop (1959) extended Terzaghi's effective stress principle to account for the presence of an air phase by intuitively introducing an average pore fluid pressure weighted over the pore air (u_a) and water (u_w) pressures, i.e.

$$\sigma' = \sigma - \left[\chi u_w + (1-\chi)u_a\right] = (\sigma - u_a) + \chi(u_a - u_w) \tag{1}$$

where σ and σ' are the total and effective stresses respectively, and χ is the weighted parameter that is arbitrarily confounded with the degree of saturation, S_r. Here, soil mechanics sign convention is used, i.e. positive stresses mean compression. Understanding the suction stress as a function of the difference between air and water pressures, as well as its dependency on the degree of saturation is a longstanding problem both theoretically and experimentally.

The present paper examines the notion of stress and its definition for a three-phase system composed of idealized soil particles and pore water menisci through a micromechanical

analysis. By considering air and water pressures, surface tension, as well as interparticle forces within an assembly of spherical particles, the (Cauchy) stress tensor can be readily calculated as a volume average of the various constituents (phases) just like in the case of a solid body consisting of interacting point masses in a volume (Love, 1944). The proposed derivation ultimately leads to a tensorial effective stress equation which can be viewed as a generalized Bishop's equation explicitly written as a function of the spatial distribution of water menisci and an anisotropic tensor describing the distribution of pore fluid around particle surfaces, including the effect of the contractile skin. It is noteworthy that the same formulation can be reached based on the theory of energy and thermodynamics.

One of the implications of this generalized formulation is that the stress tensor formulation engenders a suction based shear effect even under isotropic loading, which is fundamental to the understanding of the strength behaviour of unsaturated soils. Furthermore, as a by-product of this micromechanical derivation, an analytical expression is obtained for the weighting parameter χ. By considering regular spherical particle assemblies such as in two-particle or multi-particle configurations with tetrahedral and cubical packings, together with changing the geometry of the pore water meniscus to mimic filling, the relationship between χ and degree of saturation can be computed explicitly. The variation of χ as a material parameter with the degree of saturation on both water meniscus and particle packing is discussed in the light of experimental data already available for different types of soils. The work constitutes a rational approach within which the role of capillary forces and their distributions can be accounted for through the microscale physics that governs the state of stress in an unsaturated soil and its macroscopic engineering properties.

2. STRESS DERIVATION IN A THREE-PHASE SYSTEM

The stress tensor in a representative elementary volume (REV) comprising an ensemble of interacting solid particles in the presence of a water and air phase can be generally written as a volume average of each individual phase stress over the total volume *V*, i.e.

$$< \sigma_{ij} >= \frac{1}{V}\int_V \sigma_{ij} dV = \frac{1}{V}\sum^{N}\int_{V^p} \sigma_{ij} dV + \frac{V^w}{V} u_w \delta_{ij} + \frac{V^a}{V} u_a \delta_{ij} \tag{2}$$

where V^α, $\alpha = p, a, w$ represent solid particle, water and air phase volume respectively, N the number of particles, and δ_{ij} the Kronecker delta. In Eq. (2), the stress in the water and air phases have been considered to be hydrostatic and equal to u_w and u_a respectively. As a result, the last two terms on the right in Eq. (2) simply refer to the partial pressures due to air and water phases with their respective volume fractions applied to each individual pressure.

Next, suppose the above system is idealized as an ensemble of mono-disperse spherical particles of radius R joined by independent concave liquid bridges with negligible interparticle contact area. Since we are primarily interested in the transport of forces in the REV, we will focus on the first term on the right in Eq. (2) related to particle interactions. Applying Gauss' divergence theorem to the latter term for the case of static and weightless media, the following so-called granular stress tensor is obtained:

$$< \sigma_{ij} >_g = \frac{1}{V}\sum^{N}\int_{V^p} \sigma_{ij} dV = \frac{1}{V}\sum^{N}\int_{\Gamma^p} x_i t_j d\Gamma \tag{3}$$

where Γ^p is the surface of a particle, x_i the spatial position of points on Γ^p at which various surface tractions t_j act. Among the various surface tractions exerted on an individual particle, we will find contributions from pair-wise particle contact forces due to external loading, actions of air and water pressures on dry (Γ_d^p) and wetted (Γ_w^p) surfaces respectively, and surface tension arising from air/water/solid interfaces formed by water menisci along contour Γ_m as illustrated in Fig. 1.

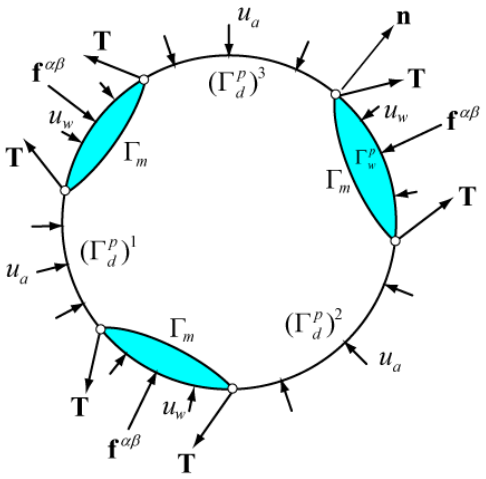

$$\Gamma_d^p = (\Gamma_d^p)^1 \cup (\Gamma_d^p)^2 \cup (\Gamma_d^p)^3$$

Figure 1 Free body diagram for analysis of interparticle forces

Furthermore, noting that $x_i = x_i^c + Rn_i$, where x_i^c is the position vector of the particle centroid, and considering equilibrium of forces on the closed surface of each particle, we finally get:

$$< \sigma_{ij} >_g = \frac{1}{V}\sum_{\alpha\beta}^{N} f_j^{\alpha\beta} l_i^{\alpha\beta} + \frac{u_a.R}{V}\sum^{N}\int_{\Gamma_d^p} n_j n_i d\Gamma + \frac{u_w R}{V}\sum^{N}\sum^{L}\int_{\Gamma_w^p} n_j n_i d\Gamma - \frac{R}{V}\sum^{N}\sum^{L}\int_{\Gamma_m} T_j n_i d\Gamma \quad (5)$$

where n_j is the normal to the particle surface, $f_j^{\alpha\beta}$ is the mutual contact force between particle pair α and β, $l_i^{\alpha\beta}$ the so-called branch vector defining to the separation distance between the same two particles, T_j the surface tension forces per unit length related to water menisci action on Γ_m formed by the intersection of the water meniscus with the particle's surface, L the number of liquid bridges, Γ_w^p is the part of the particle wetted by the liquid bridge, whereas Γ_d^p is the union of all dry parts of the particle's surface (see Fig. 1). Interestingly, the air/water interface at the particle's surface, seen as a contractile skin, allows the REV to withstand tensile stresses.

It should be noted that the decomposition of surface tractions as laid out in Fig. 1 and which enters Eq. (5) leads to the well-known result that capillary forces arising from a concave liquid bridge between two spherical particles have two sources. The first source comes from the pressure difference between air and water described by the Young-Laplace equation, whereas the second source originates from the surface tension force acting on the boundary of the wetted area on the particle surfaces where solid, air and water coexist (e.g. see Megias-Alguacil and Gauckler, 2009).

The tensor moment of force, defined by the first term to the right of Eq. (5) as a dyadic product between $\mathbf{f}$ and $\mathbf{l}$, is easily identified as the effective stress tensor σ'_{ij} used in the fully saturated case. Therefore, further rearrangement of Eq. (5) and substitution into Eq. (2) finally leads to the form of a generalized Terzaghi's effective stress relation:

$$\sigma'_{ij} = (\sigma_{ij} - u_a\delta_{ij}) + (u_a - u_w)\phi S_r\delta_{ij} + (u_a - u_w)\frac{R}{V}\sum^{N}\sum^{L}\int_{\Gamma_w^g} n_j n_i d\Gamma + \frac{R}{V}\sum^{N}\sum^{L}\int_{\Gamma_m} T_j n_i d\Gamma \quad (6)$$

in which ϕ is the porosity, S_r is the degree of saturation, whereas the last two terms relate to distributional descriptions of liquid bridges (menisci) and contractile skin effects respectively as surface integrals of dyadic products of contact normals and surface tension forces as illustrated in Fig. 2.

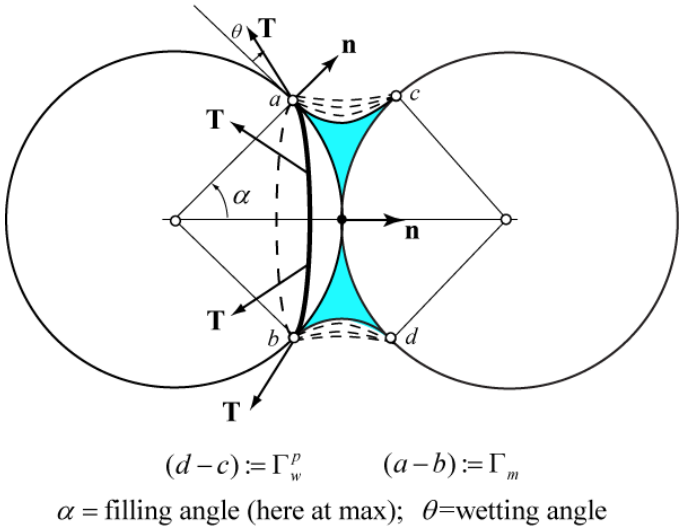

Figure 2. Geometry of meniscus and surface tension forces for a pair of spherical particles

These integrals over each pair of particles can be readily calculated and as their contributions are assembled over the entire REV, we get the following general relationships distinguishing isotropic from deviatoric components:

$$\sum^{N}\sum^{L}\int_{\Gamma_w^p} n_j n_i d\Gamma = \frac{\pi R^2}{3}(\omega\delta_{ij} + A_{ij}) \quad \text{and} \quad \sum^{N}\sum^{L}\int_{\Gamma_m} T_j n_i d\Gamma = \pi\gamma R\sin\alpha(\varpi\delta_{ij} + B_{ij}) \quad (7)$$

in which γ is the surface tension, A_{ij} and B_{ij} are deviatoric so-called fabric tensors with respect to liquid bridge arrangements, whereas ω and ϖ are parameters corresponding to their isotropic part respectively.

Finally, substituting Eq. (7) into (6) and after rearranging leads to some form of equation that is recognizable as a generalized Bishop's equation, i.e.

$$\sigma'_{ij} = (\sigma_{ij} - u_a\delta_{ij}) + \chi(u_a - u_w)\delta_{ij} + \kappa\delta_{ij} + G_{ij} \quad (8)$$

where

$$\chi = \phi S_r + \frac{V^p}{4V}\omega;\ \kappa = \frac{\pi R^2}{V}\gamma\varpi\sin\alpha;\ G_{ij} = (u_a - u_w)\frac{V^p}{4V}A_{ij} + \frac{\pi R^2}{V}B_{ij}\gamma\sin\alpha \tag{9}$$

in which α is the filling angle attached to a water meniscus.

As discussed earlier, the current derivation inherently accounts for capillary forces that arise from the pressure difference between air and water, and surface tension force acting on the wetted surface on the surface of grains, i.e. the contractile skin. Therefore, referring to Eq. (9), the term κ refers to the isotropic part of the distribution of surface tension forces with its anisotropic (deviatoric) part represented by the second term of the tensor $\mathbf{G}$. It turns out that the latter term is of second order (since $\gamma R^2 / V$ is small) relative to the first term of $\mathbf{G}$ which describes the anisotropic distribution of capillary forces due to pressure difference between air and water. In other words, the effect of capillary forces in unsaturated soils is mostly controlled by the contribution due to air-water pressure difference. Accordingly, Eq. (8) can be simply written as

$$\sigma'_{ij} = (\sigma_{ij} - u_a\delta_{ij}) + \chi(u_a - u_w)\delta_{ij} + \bar{G}_{ij},\ \text{with}\ \bar{G}_{ij} = (u_a - u_w)\frac{V^p}{4V}A_{ij} \tag{10}$$

The micromechanically derived Eq. (8) shows that the effective stress in unsaturated soil is governed by not only two independent state variables: net normal stress $(\sigma_{ij} - u_a\delta_{ij})$ and matric suction $(u_a - u_w)$ including a material variable χ as in Bishop (1959), but also by distributions of contractile skin surface tension and matric suction. Since the latter distribution can be anisotropic depending on liquid bridge spatial distribution and particle packing, effective stresses can also be affected by deviatoric loading. Turning to Eq. (9), the derived effective stress parameter χ emerges as a function of degree of saturation as well as distributional quantities such as particle packing and number of meniscus per unit volume of REV. This will be investigated in the next section as to the capturing of the dependency of χ on the degree of saturation and other parameters.

3. EFFECTIVE STRESS COEFFICIENT FOR SIMPLE PACKINGS

The effective stress parameter χ, as a function of degree of water saturation S_r, is theoretically evaluated for two limiting cases, namely simple cubic (SC) simple packing (loosest state) and tetrahedral (TH) packing (densest state) in idealized soil comprised of mono-sized spherical particles. Figures 2a,b show simple cubic and tetrahedral packing geometries respectively with liquid bridges between each pair of particles. The water meniscus is assumed to be a surface of revolution with constant curvature and circular in section so as to form a toroid. In all subsequent calculations, a small wetting angle $(\theta = 0.5°)$ is chosen to maximize the filled volume of menisci and hence achieve high degrees of saturation in the pendular regime. The effect of contact angle could be explored, but this is not the focus of this paper.

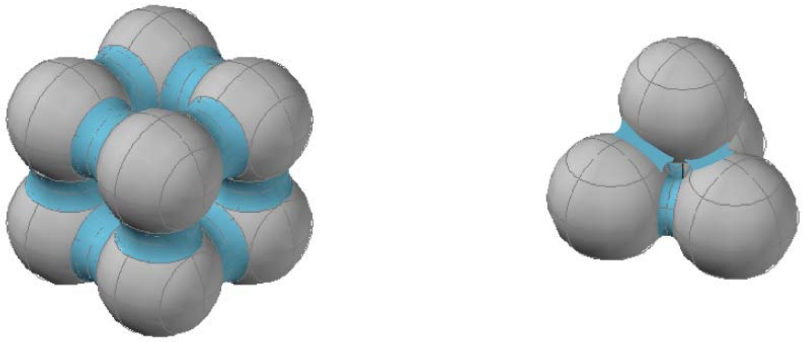

(a) simple cubic (SC) (b) tetrahedral (TH)

Figure 2. Loosest and densest packings with interconnecting water menisci

3.1 Calculation of χ

Referring back to Eqs. (6) & (7), the effective stress parameter χ emerges as the isotropic part of the integral giving the distribution of liquid bridges. For each meniscus connecting a pair of particles, we readily compute the fabric tensor as

$$F_{ij} = \int_{\Gamma_w^p} n_j n_i d\Gamma = \frac{\pi R^2}{3} \begin{bmatrix} \lambda_1 & 0 & 0 \\ 0 & \lambda_2 & 0 \\ 0 & 0 & \lambda_2 \end{bmatrix}; \ \lambda_1 = 2(1-\cos^3\alpha) \text{ and } \lambda_2 = (1-\cos\alpha)^2(2+\cos\alpha) \quad (11)$$

According to Eq.(11), F_{ij} is a symmetric tensor with its first invariant, $\delta_{ij} trace(\mathbf{F})$, being independent of the rotation of the coordinate system. Thus, referring to Eq. (7) and summing contributions of the fabric tensors over all liquid bridges on all particles, and then taking into account the isotropic part of the resultant tensor we finally find $\omega = 2L(\lambda_1 + 2\lambda_2)/3$ for different packings. Furthermore, noting Eq. (9), the explicit expression of the effective stress parameter for different packings of spherical particles can be thus derived, i.e.

$$\chi = \phi S_r + \frac{2\pi R^3}{9V} L(\lambda_1 + 2\lambda_2) = \phi S_r + (1-\phi)\frac{L}{6N}(\lambda_1 + 2\lambda_2) \quad (12)$$

which depends on the filling angle α, among others.

Using a toroidal meniscus geometry, the volume of the liquid bridge between two contacting spherical particles can be readily calculated based on α at equilibrium conditions during saturation, see Megias-Alguacil and Gauckler (2009). Therefore, χ as given in Eq. (12) can be readily calculated as a function of S_r. The maximum degree of saturation is reached whenever the filling angle reaches its maximum and the curvature of the meniscus decreases to a minimum so that the toroid degenerates into a cylinder. For example for a packing of two particles, this would give a value of $S_r = 28\%$.

Furthermore, the maximum degree of saturation for SC and TH cases can be reached without any of the liquid bridges overlapping, which can be readily calculated based on the maximum filling angle. Table 1. summarizes the results for the these packings.

Table 1. Expressions of χ for various packings

Packing	Porosity ϕ	$\mu = L / N$	χ	Maximum α	Maximum S_r
A pair of particles	0.4764	1/2=0.5	$\phi S_r + \frac{2\pi R^3}{9V}(\lambda_1 + 2\lambda_2)$	90°	28%
Tetrahedral (TH)	0.1285	6/4=1.5	$\phi S_r + 6\left(\frac{2\pi R^3}{9V}\right)(\lambda_1 + 2\lambda_2)$	30°	25%
Simple Cubic (SC)	0.4764	12/8=1.5	$\phi S_r + 12\left(\frac{2\pi R^3}{9V}\right)(\lambda_1 + 2\lambda_2)$	45°	17%

4. DISCUSSIONS AND CONCLUSIONS

Figure 4 shows the computed effective stress values as a function of degree of saturation with the line $\chi = S_r$ also plotted here as a reference. All simulations produce a curve that plots above the $\chi = S_r$ line showing a perceptible bend with a break in slope at some characteristic degree of saturation when the water meniscus reaches its maximum filling angle $\alpha_{\max}$. Subsequent filling would then proceed at fixed wetting points on the particle while the curvature of the meniscus (dotted lines in Fig. 2) continues to decrease towards reaching a larger water volume.

The simulations reveal that both packing and the number of liquid bridges influence the shape of the χ vs. S_r curve. For instance, the tetrahedral packing gives much lower χ values than those associated with the simple cubic packing for the same degree of saturation. Also, as one would expect for the same packing with decreasing number of liquid bridges, lower values of χ are predicted for the same degree of saturation because of a decrease in overall suction. We recall that overall suction depends on χ as is evident in Eq. (10) or in Bishop's original equation.

Experimental data for various types of soils are shown in Fig. 5 for comparison with the numerical results of Fig. 4. It should be noted that the range of degree of saturation, examined in the numerical computations based on idealized mono-sized spheres, is well below 30% since the menisci are not allowed to merge to give full saturation. The restriction of the packing to rather simple configurations with mono-sized spherical particles could plausibly account for the difference between experimental and computed data. This matter will require a more detailed investigation. At any rate, it is also not evident that the experimental data in the range of small degree of saturation investigated (less than 30%) is accurate and reliable, given known difficulties in measuring low suction in soils.

The theory developed in this paper is being extended to poly-disperse and non-spherical particles, which should give more realistic χ vs. S_r curves. Given the limited experimental data for low to extremely low suctions on soils, discrete element simulations is an alternative means for exploring, among other things, the validity of the proposed theory. Another interesting outcome of this work arising from Eq. (10) is that the contribution of the matric suction to the effective stress is by no means isotropic, but is generally anisotropic as dictated by the spatial distribution of liquid bridges and fabric of the solid skeleton during deformation history. It is thought that this issue becomes particularly relevant in the pendular regime where material instabilities in the form of skeleton collapse are common. (ref). Indeed, discrete element numerical simulations may be of great value for elucidating volume

changes in unsaturated soils as a result of increase or decrease in water saturation and also for formulating constitutive models for unsaturated soils.

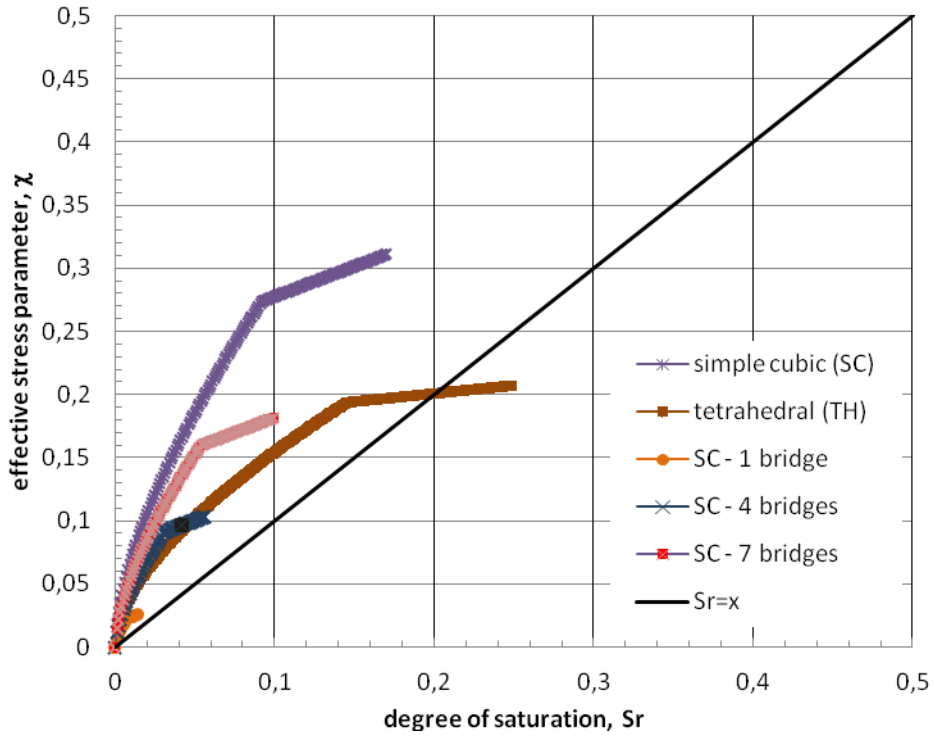

Figure 4. Computed relationship between degree of saturation *Sr* and effective stress parameter χ

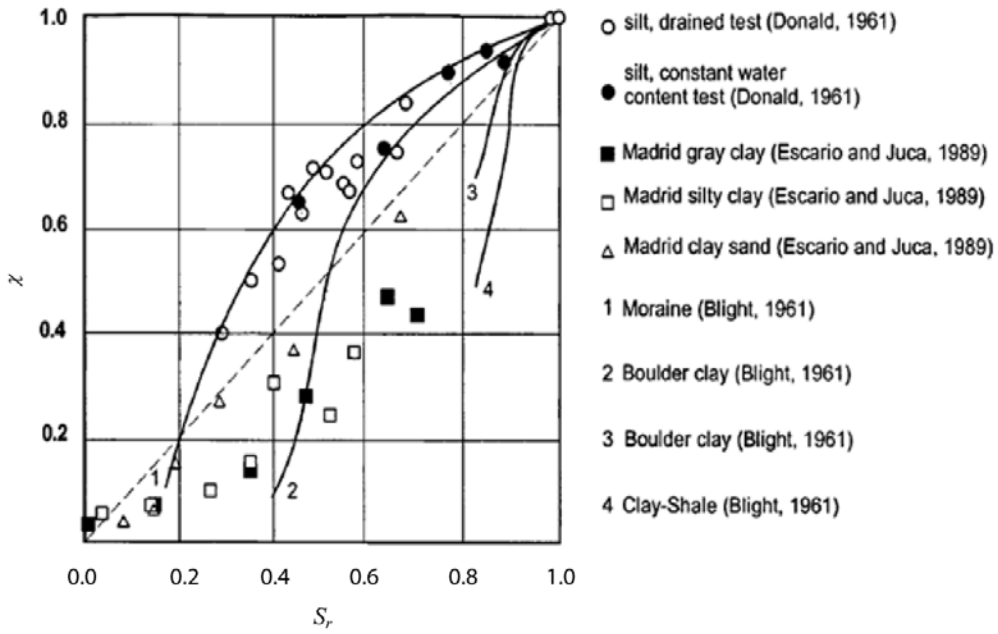

Figure 5. Relationship between degree of saturation *Sr* and effective stress parameter χ for various soils (After Bishop, 1961?)

ACKNOWLEDGEMENTS

The first two authors are grateful to funding provided by the Natural Science and Engineering Science Research Council and Computer Modelling Foundation. The third author is grateful for funding provided by the CEMAGREF in the form of a research visit fellowship to Calgary in summer 2010.

REFERENCES

Bishop, A.W. (1959), “The principle of effective stress”. Teknisk Ukeblad, 106(39): 859-863.

Bishop, A.W. (1961), “Some aspects of effective stress in saturated and partially saturated soils”. Géotechnique, 13(3): 177-197.

Love, A. E. H. (1944). Theory of Elasticity, 4th. Ed. Dover, New York.

Megias-Alguacil, D. & Gauckler, L.J. (2009), "Capillary forces between two solid spheres linked by a concave liquid bridge: regions of existence and forces mapping". J. AIChE, 55(5): 1103-1109.

Ning, L. & Griffiths, D.V. (2004),”Profiles of steady-state suction stress in unsaturated soils”. J. Geotech. Geoenviron, 130(10): 1063-1076.

Scholtès, L., Hicher, P.-Y., Nicot, F., Chareyre, B. and Darve, F. (2009), “On the capillary stress tensor in wet granular materials”. International Journal for Numerical and Analytical Methods in Geomechanics, 33: 1289–1313. doi: 10.1002/nag.767